OPTOELECTRONICS AND ADVANCED MATERIALS – RAPID COMMUNICATIONS Vol. 7, No. 11-12, November - December 2013, p. 849-855

Synthesis and photovoltaic properties of carbazole-based conjugated polymers

YUANCHENG QIN*, SHA LENG, DAN ZHOU, WEILI DAI, MINGJUN LI, XINGHUA TANG, YU XIE
Key Laboratory of Jiangxi Province for Persistant Pollutants Control and Resources Recycle, Nanchang Hangkong University, Nanchang, 330063, P. R. China

Two kinds of copolymers based on dihydroindolo[3,2-b]carbazole in combination with dithieno[3,2-b:2',3'-d]silole (P1) and cyclopenta[2,1-b:3,4-b']dithiophene (P2) were designed and synthesized. The structures and properties of the copolymers were fully characterized. Compared with P1 film, P2 film showed a slighted red-shifted absorption spectrum. The two polymers had similar lowest unoccupied molecular orbital energy levels (3.6-3.7 eV); however, there were differences in highest occupied molecular orbital energy level: -5.54 eV for P1 and -4.92 eV for P2. These results indicate that it is a simple and effective approach to tune the bandgap in a conjugated polymer by tune the bridge atom.

(Received January 6, 2013; accepted November 7, 2013)

Keywords: Carbazole, Conjugated Polymers, Organic solar cells, Photovoltaic properties

1. Introduction

Polymeric solar cells (PSCs) have attracted considerable attention over the past several years due to their unique advantages of low cost, light weight, flexibility, tunability with respect to light-harvesting capabilities and great potential for realization of large-area devices [1-3]. Bulk heterojunction solar cells (BHSCs), with an active layer comprising an interpenetrating network of conjugated polymers as the electron donor and fullerene as electron acceptor, [4-7] have been extensively studied and display the highest effeciencies to date in PSCs. The synthesis of novel conjugated polymers with low band gaps, high charge carrier mobility, suitable energy levels, and broad absorptions is of important in developing high-performance PSCs. These polymers typically adopt a donor-acceptor (D-A) strategy with alternating electron-rich and electron-poor moieties along the conjugated polymer chain [8-11]. By controlling intramolecular charge transfer (ICT) between the donor and acceptor units in the D-A polymers, the band gaps can be well tuned [12].

The family of polymers based on carbazole, [13-15] especially alkyl substituted moieties, attracted our interest because of their distinctive performance as a common unit in PSCs that can achieve power conversion efficiencies (PCEs) higher than 6% [16]. The polymers bearing carbazole unit exhibit the advantages of good solubility properties, high hole mobility and air stable features, originating from the nature of the carbazole unit, such as rigid biphenylunit, delocalization of the lone electron pair of nitrogen atom over aromatic structure [17]. Particularly, easy modification of N-H bond of carbazole can allow us to improve the solubility and photoelectric properties for carbazole-containing polymers.

Recently, heteroaromatic structures based on biphenyl or bisthiophene with a bridging atom (C, Si, or N) have been widely estimated [18-24]. Particularly, electron-rich units bridged bithiophene-based conjugated polymers such as dithieno[3,2-b:2',3'-d]silole [25-26] and cyclopenta[2,1-b:3,4-b']dithiophene (CPDT) [27-28] have been considered with growing interest by various research groups derive from their good electron-donating properties, rigid coplanar structure with easy π–π* intermolecular interactions [29]. Furthermore, the merit of functionalization at bridging carbon and silicon allows for introducing highly solubilizing aliphatic side chains without decrease its coplanarity.

In this work, we therefore present new alternating copolymers based on dithieno[3,2-b: 2', 3'-d]silole, cyclopenta [2,1-b:3,4-b']dithiophene carbazole derivatives moieties, namely P1 and P2 (as seen in Chart 1). The effects of the different segments on the absorption spectra, the energy levels, and the photovoltaic performance of the resulting carbazole-based copolymers were well investigated in this paper.

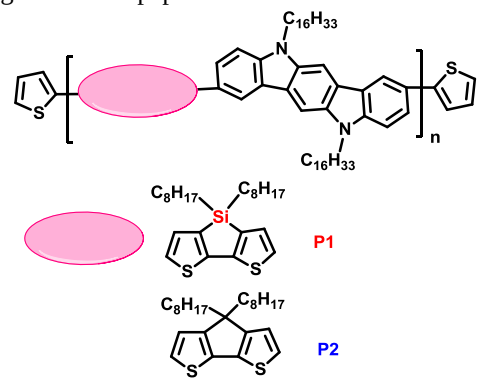

Chart 1. Structures of the Low Band Gap Copolymers P1, P2 and P3.

2. Experimental

2.1. Materials

All chemical reagents were purchased from Acros, TCI and Aldrich Chemical Co. and were used as received, unless stated otherwise. All solvents were distilled over appropriate drying agent(s) prior to use and were purged with nitrogen. All manipulations involving air-sensitive reagents were performed in a dry argon. (4-Bromophenyl)hydrazine hydrochloride, [30] 1, 4-bis(2-(4-bromophenyl) -hydrazono)cyclohexane, [31] [3,2-b:2',3'-d]silole [32] and 4,4′-dioctyl-4H-cyclopenta[2,1-b:3,4-b']dithiophene [33] were synthesized similar to already published procedures.

2.2 Instrumentation

The nuclear magnetic resonance (NMR) spectra were collected on a Bruker ARX 400 NMR spectrometer with deuterated chloroform as the solvent and with tetramethylsilane (δ=0) as the internal standard. Cyclic voltammetry (CV) measurements were performed on an eDAQ potentiostat electrochemical analyzer using a three-electrode cell with a platinum plate working electrode, a platinum wire counter electrode, and Ag/AgCl (0.1 mol/L) reference electrode at a scan rate of 50 mV/s. Tetrabutylammonium hexafluorophosphate (Bu_4NClO_4) in an anhydrous and nitrogen-saturated acetonitrile (CH_3CN) solution (0.1 mol/L) was used as the supporting electrolyte. Polymers to be measured were coated on the platinum plate working electrodes from dilute chloroform solutions. UV-vis and fluorescence spectra were recorded on a PerkinElmer Lambda 900 UV-vis/NIR spectrometer and a PerkinElmer LS 55 spectrometer, respectively. Thermogravimetric analyses (TGA) were conducted on a TA Instruments Model TGA Q500 thermogravimetric analyzer at a heating rate of 10 °C min under N_2 flow (90 mL/min). Current-voltage (*J-V*) characteristics were recorded using Keithley 2400 Source Meter in the dark and under 100 mW/cm^2 simulated AM 1.5 G irradiation (Abet Solar Simulator Sun2000).

2.3 Device fabrication and characterization

Solar cell was fabricated on an indium tin oxide (ITO)-coated glass substrate in the following structure. Prior to use, the ITO glass substrate was ultrasonicated for 20 min in acetone and cleaned with deionized water and 2-propanol, and subsequently dried under a stream of nitrogen and subjected to the treatment of UV ozone over 30 min. The poly(3, 4-ethylenedioxythiophene): polystyrenesulfonate (PEDOT:PSS) was spin-cast from aqueous solution (4000 rpm for 30 s) on top of the ITO to serve as a hole-only transport layer. The PEDOT:PSS layer was subsequently annealed in air at 140 °C during 10min. On top of this PEDOT:PSS film, a layer of a blend of polymer:PC61BM (1:2, w/w) was spin-coated from dichlorobenzene solution. A 1 nm layer of LiF followed by a 100 nm layer of Al were evaporated under vacuum (<10^{-6} Torr) to form the electrodes. The thicknesses of all the films were measured by a Dektak profiler. Current-voltage (*J-V*) characteristics were recorded using Keithley 2400 Source Meter in the dark and under 100 mW/cm^2 simulated AM 1.5 G irradiation (Abet Solar Simulator Sun 2000).

2.4 Synthesis of the monomer

The synthesis and structure of the monomer are outlined in Scheme 1.

2, 8-dibromo-5,11-dihexadecyl-5,11-dihydroindolo [3,2-b]carbazole (M1) [34]. NaH (0.25g) was added in portions to a solution of compound 3 (2.57g) in 9 mL of anhydrous dimethylformamide (DMF) in a 50 mL three-neck flask under N_2 atmosphere at room temperature. After 10 minutes, when the reaction mixture turned into a blood red suspensions, the mixture was stired for another 30 minutes and 6mL bromohexadecane was added. The color of the mixture was subsequently from red to yellow, the system kept at room temperature for 24h before being poured into 300 mL CH_3OH and filtered. The organic phase was then washed with water and CH_3OH (3× 100 mL). The organic phase was dried ($MgSO_4$) and the solvent evaporated under reduced pressure. The crude product was purified through column chromatography (SiO_2, hexane /CH_2Cl_2 1:1) to obtain monomer M1 as a yellow solid (1.20 g, 36.00%, mp: 60–61 °C). ^{1}H NMR (400 MHz, $CDCl_3$, δ/ppm): 8.51 (m, 2H, Ph-H), 7.97 (m, 2H, Ph-H), 7.43 (s, 2H, thiophene-H), 2.66 (t, 4H, thiophene-CH_2), 1.66 (m, 4H, CH_2), 1.33 (t, 36H, CH_2), 0.87 (t, 6H, CH_3). ^{13}C NMR (100 MHz, $CDCl_3$, δ/ppm): 151.5, 143.0, 138.6, 132.7, 130.7, 125.7, 124.8, 114.1, 31.9, 29.8, 29.8, 29.7, 29.7, 29.7, 29.6, 29.5, 29.4, 29.3, 22.7, 14.2.

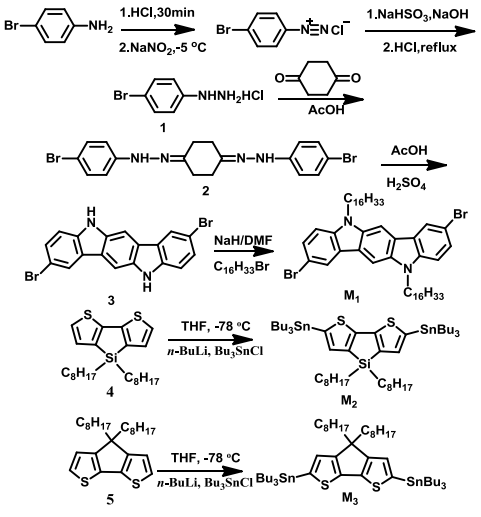

Scheme 1. Synthetic route for monomers.

4,4′-dioctyl-5,5′-bis(trimethyltin)-dithieno[3,2-b:2',3'-d]silole (M2) [35]. To a solution of compound 4 (1.47 g, 3.52 mmol) in anhydrous THF (41 mL) was added n-BuLi (3.60 mL, 2.5 M in hexanes) dropwisely at -78 °C. The reaction mixture was subsequently warmed to room

temperature and stirred at room temperature for 2.0 h. The solution was cooled down to –78 °C and 2.90 g Bu_3SnCl in 2 mL THF was added dropwisely. The reaction mixture was subsequently warmed to room temperature and stirred overnight. The solution was extracted three times with Et_2O, washed with water, dried over $MgSO_4$, and the solvent was evaporated. And the crude product was purified by column chromatography to yield a black solid (1.78 g, 74.40% yield). ^{1}H NMR ($CDCl_3$, 400Hz, δ/ppm): 7.05 (s, 2H, thiophene-H), 1.60 (t, 12H, *J*=4.00 Hz, $SnCH_2$), 1.41-1.30 (m, 16H, CH_2), 1.28-1.02 (m, 32H, CH_2), 0.91-0.85 (m, 28H, $SiCH_2$, CH_3). ^{13}C NMR ($CDCl_3$, 100MHz, δ/ppm): 154.96, 142.89, 137.94, 136.52, 129.63, 33.20, 31.90, 29.22, 29.10, 29.00, 28.89, 27.55, 27.26, 26.97, 24.33, 24.26, 22.66, 14.11, 13.67, 12.64, 12.56, 12.05, 11.95, 10.88, 9.19.

(4,4-dioctyl-cyclopenta[1,2-b:5,4-b']dithiophene-2,6-diyl)bis(tributylstannane) (M3) [36]. To a solution of compound 5 (1.0g，2.48mmol) in anhudrous THF (30 mL) was added n-BuLi (2.46 mL, 2.5 M in hexanes) dropwisely at -78 °C. The solution was stirred at -78 °C for 0.5 h. Then, the mixture was subsequently warmed to room temperature and stirred at room temperature for 2.0 h. The solution was cooled down to –78 °C and 1.86g Bu_3SnCl (5.71mmol)in 2 mL THF was added slowly. The solution was stirred for 0.5 h. The reaction mixture was warmed to room temperature and stirred overnight. The mixture was extracted two times with CH_2Cl_2, washed with water, dried over $MgSO_4$, and the solvent was evaporated. The crude product was then purified by column chromatography (silica gel, hexane) yielding the title compound as a yellow oily liquid (1.97 g, 81% yield). ^{1}H NMR ($CDCl_3$, 400Hz, δ/ppm): 6.9 (s, 2H, thiophene-H), 1.80 (t, 4H, *J*=8.00 Hz, CCH_2), 1.60 (t, 12H, *J*=3.44 Hz, $SnCH_2$), 1.39-1.23 (m, 16H, CH_2), 1.21-1.13 (m, 24H, CH_2), 1.11-0.98 (m, 8H, CH_2), 0.91-0.83 (m, 24H, CH_3). ^{13}C NMR ($CDCl_3$, 100MHz, δ/ppm): 160.27, 142.27, 135.82, 129.71, 52.04, 37.79, 31.86, 30.09, 29.40, 29.28, 29.12, 29.01, 28.91, 27.51, 27.23, 26.95, 24.65, 22.65, 14.11, 13.70, 10.90.

2.5 Polymerization

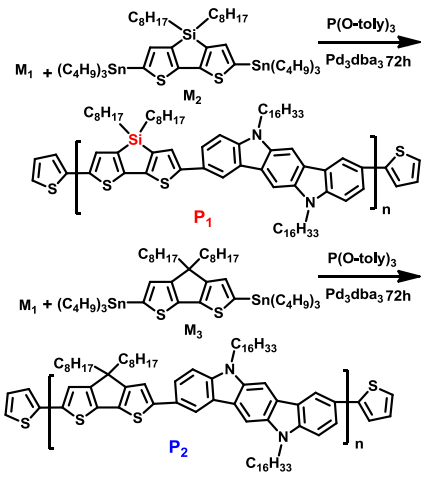

Scheme 2. Synthetic route for copolymers.

The synthesis and structures of the copolymers are outlined in Scheme 2. A typical experimental procedure for the polymerization of monomer M1 and monomer M2 was as follows:

P1: Under argon atmosphere, monomer M1 (0.27 mmol, 0.2330g) and monomer M2 (0.27 mmol, 0.2691g) were dissolved in 13.5mL mL of toluene. The solution was flushed with argon for 10 min, and then Pd_2dba_3 (4.90mg) and P(o-tolyl$_3$)(6.60 mg, 8%) were added into the flask. The flask was purged three times with successive vacuum and argon filling cycles. The polymerization reaction was heated to 110 °C, and the mixture was stirred for 72 h under argon atmosphere. 2-Tributylstannyl thiophene (21.00μL) was added to the reaction. After two hours, 2-bromothiophene (7.00 μL) was added. The mixture was stirred overnight to complete the end-capping reaction. The mixture was cooled to room temperature and poured slowly in 350 mL of methanol. The precipitate was filtered and washed with methanol and hexane in a soxhlet apparatus to remove the oligomers and catalyst residue. Finally, the polymer was extracted with chloroform. The solution was condensed by evaporation and precipitated into methanol. The polymer was collected as a dark purple solid with a yield of 19% (96 mg). ^{1}H NMR ($CDCl_3$, 400Hz, δ/ppm): ^{1}H NMR ($CDCl_3$, 400Hz, δ/ppm): 8.27-6.24 (m, 10H, thiophene-H, Ph-H), 5.02-4.28 (t, 4H, NCH_2), 3.0-0.83 (m, 96H, CH_2, CH_3).

P2: P2 was synthesized from monomers M1(0.27 mmol, 0.2330) and M3 (0.27 mmol, 0.2648g) as a dark purple solid with a yield of 44% according to the method of polymer P1 described above. ^{1}H NMR ($CDCl_3$, 400Hz, δ/ppm): 8.20 (d, 2H, *J*=8.00 Hz, Ph-H), 8.06 (d, 2H, *J*=4.00 Hz, Ph-H), 7.78 (s, 2H, Ph-H), 7.46 (s, 2H, Ph-H), 6.95 (s, 2H, thiophene-H), 4.45 (t, 4H, NCH_2), 2.04 (t, 4H, *J*=5.36 Hz, CCH_2), 1.85-1.24 (m, 80H, CH_2), 0.98 (t, 12H, *J*=3.80 Hz, CH_3).

3. Results and discussion

3.1 Synthesis of monomers and polymers

The synthesis of the carbazole-based monomer (M1) is shown in Scheme 1. The intermediate compounds (4-bromophenyl)hydrazine hydrochloride, [30] 1, 4-bis(2-(4-bromophenyl)hydrazono)cyclohexane, [31] [3,2-b:2',3'-d]silole [32] (4) and 4,4′-dioctyl-4H-cyclopenta[2,1-b:3,4-b']dithiophene [33] (5) were synthesized according to the published procedures. Monomer M2 and M3 were prepared by compound 4 or 5 with tributylchlorostannane and *n*-butyllithium, respectively. The chemical structures of all the three monomers were confirmed by ^{1}H NMR and ^{13}CNMR.

The carbazole-based conjugated copolymers P1 and P2 were prepared by Stille coupling reactions with an equivalently molar ratio of the dibromro derivatives (M2) and distannyl of 4,4′-dioctyl-5,5′-bis(trimethyltin)-dithieno[3,2-b:2',3'-d]silole or (4,4-dioctyl-cyclopenta[1,2-b:5,4-b']dithiophene-2,6-diyl)bis(tributylstannane) compounds, as illustrated in Scheme 2. All the two

polymers can partially dissolve in common solvents such as chloroform, toluene, chlorobenzene, and tetrahydrofuran, etc., showing the special contribution of the alkyl substitutions on carbazole to the solubility of the copolymers. Molecular weights and polydispersity indices (PDIs) of the polymers, as shown in Table 1, are determined by gel permeation chromatography (GPC) analysis with a polystyrene standard calibration. Number-average molecular weight (*M*n) of polymers P1 and P2 were found to be 24000 and 9000 g/mol, respectively, with the corresponding polydispersity indices (PDI) of 1.83 and 1.78.

Table 1. Molecular weights and thermal properties of the polymers.

polymers	*M*w[a] (g/mol)	*M*n[a] (g/mol)	PDI[a] (*M*w/*M*n)	T_d (°C)
P1	44000	24000	1.83	368
P2	16000	9000	1.78	332

[a] *M*w, *M*n, and PDI of the polymers were determined by GPC using polystyrene standards in THF. [b] The 5% weight-loss temperatures under N_2 atmosphere.

3.2 Thermal stability

The thermal stabilities of P1 and P2 are important for device fabrication. Thermogravimetric analysis (Fig. 1) showed that that both polymer P1 and P2 exhibit good thermal stability. The onset temperatures with 5% weight loss (T_d) of P1 and P2 are 368 and 332 °C, respectively. This indicates that the copolymers are stable enough for the applications in optoelectronic devices.

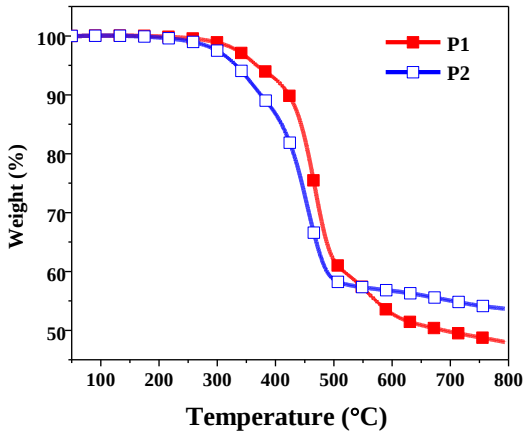

Fig. 1. TGA curves of the copolymers recorded under nitrogen at a heating rate of 10 °C /min.

3.3 Optical properties

Table 2. Optical properties of the copolymers.

polymers	UV-vis absorption spectra			
	solution[a]	film[b]		
	λ_{max} (nm)	λ_{max} (nm)	λ_{onset} (nm)	E_g^{opt} (eV)[c]
P1	339, 430	342, 429	725	1.71
P2	342, 431	349, 435	847	1.46

[a]Measured in chloroform solution. [b]Cast from chloroform solution. [c]Bandgap estimated from the onset wavelength (λ_{onset}) of the optical absorption: $E_g^{opt}=hc/\lambda_{onset}$.

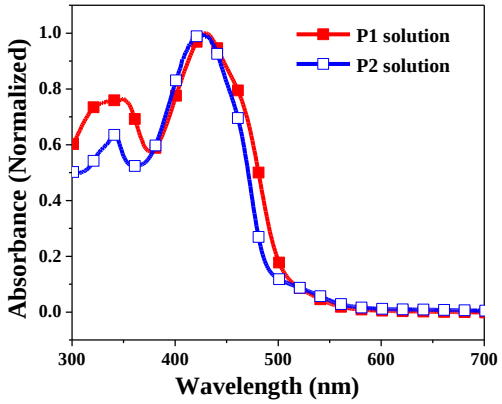

Fig. 2. Normalized UV vis absorption spectra of copolymers in chloroform solutions.

The normalized UV-vis absorption spectra of the copolymers in dilute chloroform solution and as spin-coated films on quartz substrates were investigated (Fig. 2). Table 2 summarized the optical data, including the absorption peak wavelengths (λ_{max}), absorption edge wavelengths (λ_{onset}) and the optical band gap (E_g^{opt}) calculated as $E_g^{opt}=hc/\lambda_{onset}$ (eV). The copolymers showed two absorption peaks at 339/430 nm for P1 and 342/431 nm for P2 in dilute solution UV-vis absorption spectra, which can be assigned to the π-π* transition of the conjugated polymer backbone. In addition, the absorption spectra of the two polymers in the solid film were similar to their corresponding solution spectra, with their absorption maxima at 342 and 431 nm of P1, 349 and 435 nm of P2 (shown in Fig. 3). Obviously, it's noteworthy that there is only very limited red shift for the absorption spectra of all the synthesized polymers when going from the solution to the solid state, indicating that there is no obvious aggregation or long-range orderly π-π stacking formed in the solid state. From the absorption edge wavelengths of the individual copolymer, the optical band gap of P1 was estimated to be 1.71 eV (λ_{onset}=725 nm), while smaller band gap of 1.46 eV was calculated for P2 (λ_{onset}=847 nm). In contrast to polymer P1, the slightly red-shift in UV-vis absorption spectrum and narrower optical

band gap of P2 may owing to the better coplanarity of conjugated polymer backbone.

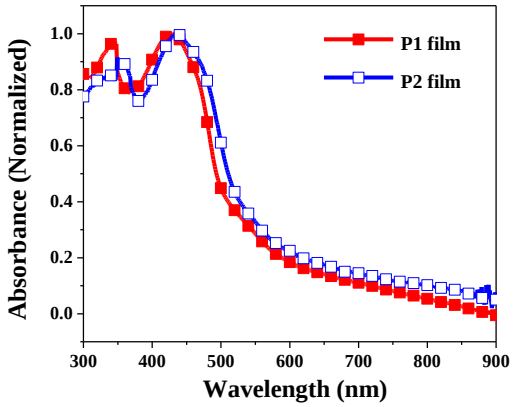

Fig. 3. Normalized UV vis absorption spectra of copolymers in solid films prepared by spin-coating from chloroform solutions.

3.4 Electrochemical properties

The positions of the lowest unoccupied molecular orbital (LUMO) and highest occupied molecular orbital (HOMO) of the copolymers exert much influence on the performance of the resulting PSCs, which can affect the driving force for charge transfer and the V_{oc} [37-38]. To determine the HOMO and LUMO levels of polymers, cyclic voltammetry (CV) measurements were performed at room temperature under nitrogen atmosphere at a scan rate of 50 mV/s. The recorded CV curves were referenced to an Ag/Ag^+ electrode, which was calibrated using a ferrocene/ferrocenium (Fc/Fc^+) redox couple (4.8 eV below the vacuum level) as an external standard. The $E_{1/2}$ of the Fc/Fc^+ redox couple was found to be 0.48 V vs the Ag/AgCl reference electrode. Therefore, the HOMO and LUMO energy levels of the polymers can be estimated using the empirical equation [39-40]:

$$HOMO=-e(E_{ox}+4.32)\ (eV)$$

$$LUMO=-e(E_{red}+4.32)\ (eV)$$

$$E_g^{EC}= e(E_{ox}–E_{red})$$

In the above equation, the E_{ox} and E_{red} stand for the onset potentials of the oxidation and reduction processes relative to the Ag/AgCl reference electrode, respectively. The cyclic voltammograms of the polymer thin films were shown in Fig. 4, and the corresponding electrochemical data were summarized in Table 3. In the anodic scan, the onsets of oxidation for P1 and P2 occurred at 1.22 and 0.63 V, which correspond to the HOMO levels of P1 and P2 values of -5.54 and -4.95 eV, respectively. Interestingly, the HOMO level of P2 was ~0.59 eV higher than that of P1, which man attribute to the stronger electron-donating ability of the cyclopentadithiophene (CPDT) unit or the delocalization of the HOMO because of better coplanarity between the cyclopentadithiophene (CPDT) and carbazole segments [41]. This was well in agree with the UV result as mentioned above. In the negative potential, the onset reduction potentials are located at -0.56 V for P1 and -0.52 V for P2 versus Ag/Ag^+. The LUMO energy levels of the polymers P1 and P2 were thus determined to be -3.76 and -3.80 eV. From the values of the cyclic voltammetry data, the electrochemical band gaps (E_g^{EC}) of P1 and P2 were calculated to be 1.78 and 1.15 eV. Thanks to the higher HOMO level, P2 exhibited narrower band gap compared to P1. This seemingly subtle structural difference can affect the levels of the polymers, with the former central atom was carbon, whereas the latter central atom was silicon.

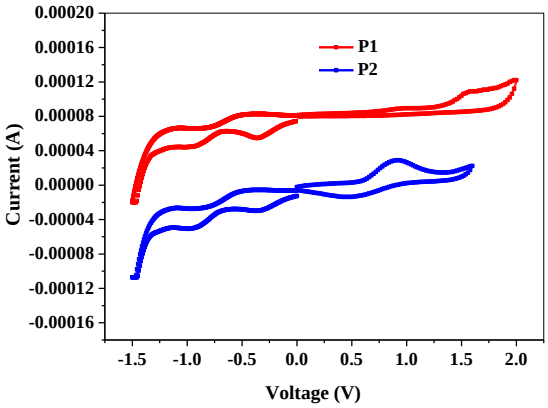

Fig. 4. Cyclic voltammograms of polymer thin films.

Table 3. Electrochemical properties of the polymers.

polymers	cyclic voltammetry		
	p-doping	n-doping	
	$[E_{ox}]^a$/HOMO^c (V)/(eV)	$[E_{red}]^b$/LUMO^d (V)/(eV)	E_g^{EC} (eV)
P1	1.22/-5.54	-0.56/-3.76	1.78
P2	0.63/-4.95	-0.52/-3.80	1.15

[a]Onset oxidation potentials measured by cyclic voltammetry. [b]Onset reduction potentials measured by cyclic voltammetry. [c]Calculated from the onset oxidation potentials, HOMO=-e(E_{ox}+4.32) eV. [d]Calculated from the onset reduction potentials, LUMO=-e(E_{red}+4.32) eV.

The energy-level diagram of the polymers and PCBM was shown in Fig. 5, the differences of the LUMO level values between the polymers and PCBM were more than 0.5 eV(>0.3 eV). Therefore, the electrons can be efficiently transported from the polymers to PCBM by an energetically downhill cascade pathway.

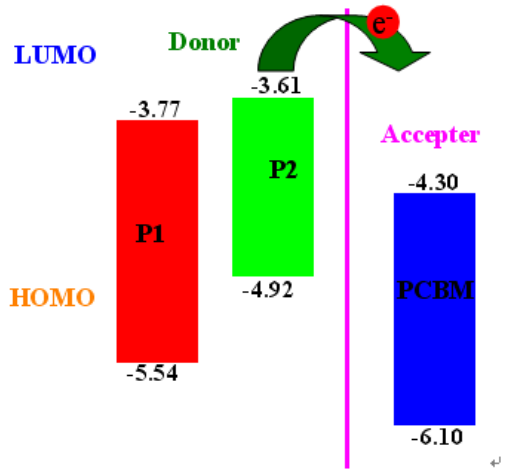

Fig. 5. Energy-level diagram showing the HOMO and LUMO energy levels from CV data of P1, P2 and PCBM.

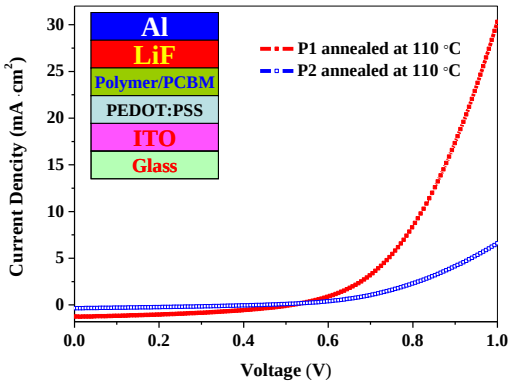

Fig. 6. J-V characteristics of photovoltaic cells based on P1-P2:$PC_{61}BM$ (1:2) under AM 1.5G illumination from a calibrated solar simulator with an intensity of 100 mW/cm ^{2}.

3.5 Photovoltaic properties

To research the photovoltaic properties of the copolymers, the bulk-heterojunction polymer photovoltaic cells with a structure of ITO/PEDOT:PSS/copolymers: PC61BM/LiF/Al (ITO, indium tin oxide; PEDOT:PSS, poly(styrene sulfonate):poly(ethylene-dioxythiophene; PC61BM, [6,6]-phenyl C61 butyric acid methyl ester) were fabricated, where the copolymers were used as donors and PC61BM as acceptor. Thin films of the polymer:PC61BM blend were prepared by using *o*-dichlorobenzene (DCB) as solvent. Fig. 6 shows the *J-V* characteristics of photovoltaic cells based on P1-P2:PC61BM (1:2) under AM 1.5G illumination from a calibrated solar simulator with an intensity of 100 mW/cm2. The photovoltaic performance of the two polymers, including the short-circuit current (*J*SC), the open-circuit voltage (*V*OC), the power conversion efficiency (PCE) and the fill factor (FF) are summarized in Table 4. The *V*OC of the device based on P1:PC61BM was 0.51 V, which was higher than that of P2:PC61BM. This difference could arise from the deeper HOMO energy level of P1 compared with the counterpart P2, since the *V*OC depends on the energy difference between the LUMO level of the acceptor (PCBM) and the HOMO level of the donor (the conjugated polymer) [42]. The device based on ITO/PEDOT:PSS/P1:PCBM (1:2, w/w)/LiF/Al exhibited a *V*oc of 0.51 V, a *J*sc of 1.25 mA/cm2, a FF of 40.00%, and a PCE of 0.30%. While, the corresponding *J*sc, *V*oc, FF and PCE values were found to be 0.35 mA/cm2, 0.44 V, 32.50%, and 0.10%, respectively for the P2/PCBM (1:2, w/w)-based device. The relative low power conversion efficiencies of the two polymers may be ascribe to the optical absorption is poor match with the solar spectrum.

Table 4. Performance of polymer solar cells[a].

active layer[b]	cathode	V_{oc} (V)	J_{sc} (mA/cm^2)	FF (%)	PCE (%)
P1	LiF/Al	0.51	1.25	40.0	0.30
P2	LiF/Al	0.44	0.35	32.5	0.10

[a]All the devices were measured under the illuminationo f AM1.5 G at 100 mW/cm^2. [b]All the weight ratios of polymer and $PC_{61}BM$ were 1:2 and annealed at 110 °C for 10 min.

4. Conclusion

In summary, two carbazole-based conjugated copolymers P1 and P2, as new polymeric donors in BHJ PVCs, were successfully synthesized via the Stille coupling reaction. All the copolymers showed good thermal stability. The energy levels and band gaps of the copolymers could be effectively modulated by replacing the bridging carbon atom in cyclopenta[2,1-b;3,4-b′]dithiophene containg polymer with silicon. Under 1.5 G illumination (100 mW/cm^2), a open-circuit voltage (V_{oc}) of 0.51 V with energy conversion efficiencies 0.30%, fill factor 40.00% and short-circuit current density (J_{sc}) of 1.25 mA/cm^2 were observed in the device based on polymer P1. The device incorporating ITO/PEDOT:PSS/P2:PCBM (1:2, w/w)/LiF/Al blend achieved a PCE of 0.1% with J_{sc} = 0.35 mA/cm^2, V_{oc} = 0.44V, and FF = 32.5%.

Acknowledgments

The work was financially supported by Aviation Science Fund of China (No: 2011ZF56017), Jiangxi Province Education Department of Science and Technology Project (No: GJJ12455) and Key Laboratory of Jiangxi Province for Persistant Pollutants Control and Resources Recycle (No: ST201222004).

References

[1] G. Dennler, M. C. Scharber, C. J. Brabec, Adv. Mater. **21**, 1323 (2009).
[2] F. C. Krebs, Sol. Energy Mater. Sol. Cells **93**, 394 (2009).
[3] J. W. Chen, Y. Cao, Acc. Chem. Res. **42**, 1709 (2009).
[4] G. Y. Sang, Y. P. Zou, Y. F. Li, J. Phys. Chem. C **112**, 12058 (2008).
[5] I. Osaka, T. Abe, M. Shimawaki, T. Koganezawa, K. Takimiya, ACS Macro Lett. **1**, 437 (2012).
[6] T. Y. Chu, J. P. Lu, S. Beaupré, Y. G. Zhang, J. R. Pouliot, S. Wakim, J. Y. Zhou, M. Leclerc, Z. Li, J. F. Ding, Y. Tao, J. Am. Chem. Soc. **133**, 4250 (2011).
[7] Y. J. He, H. Y. Chen, J. H. Hou, Y. F. Li, J. Am. Chem. Soc. **132**, 1377 (2010).
[8] R. M Duan, L. Ye, X. Guo, Y. Huang, P. Wang, S. Q. Zhang, J. P. Zhang, L. J. Huo, J. H. Hou, Macromolecules **45**, 3032 (2012).
[9] B. Burkhart, P. P. Khlyabich, B. C. Thompson, Macromolecules **45**, 3740 (2012).
[10] D. Lee, E. Hubijar, G. J. D. Kalaw, J. P. Ferraris, Chem. Mater. **24**, 2534 (2012).
[11] L. Huo, X. Guo, S. Zhang, Y. Li, J. Hou, Macromolecules **44**, 4035 (2011).
[12] S. Subramaniyan, H. Xin, F. S. Kim, S. A. Jenekhe, Macromolecules **44**, 6245 (2011).
[13] Y. H. Fu, H. Cha, G. Lee, B. J. Moon, C. E. Park, T. Park, Macromolecules **45**, 3004 (2012).
[14] A. Kimoto, Y. Tajima, Org. Lett. **14**, 2282 (2012).
[15] Y. J. Cheng, J. S. Wu, P. I. Shih, C. Y. Chang, P. C. Jwo, W. S. Kao, C. S. Hsu, Chem. Mater. **23**, 2361 (2011).
[16] J. M. Sun, Y. X. Zhu, X. F. Xu, L. F. Lan, L. J. Zhang, P. Cai, J. W. Chen, J. B. Peng, Y. Cao, J. Phys. Chem. C, **116**, 14188 (2012).
[17] Z. G. Zhang, Y. L. Liu, Y. Yang, K. Y. Hou, B. Peng, G. J. Zhao, M. J. Zhang, X. Guo, E. T. Kang, Y. F. Li, Macromolecules **43**, 9376 (2010).
[18] P. L. T. Boudreault, A. Michaud, M. Leclerc, Macromol. Rapid Commun. **28**, 2176 (2007).
[19] M. Svensson, F. Zhang, S. C. Veenstra, W. J. H. Verhees, J. C. Hummelen, J. M. Kroon, O. Inganaes, M. R. Andersson, Adv. Mater. **15**, 988 (2003).
[20] E. Wang, L. Wang, L. Lan, C. Luo, W. Zhuang, J. Peng, Y. Cao, Appl. Phys. Lett. **92**, 033307/1 (2008).
[21] N. Blouin, A. Michaud, M. Leclerc, Adv. Mater. **19**, 2295 (2007).
[22] A. J. Moule, A. Tsami, T. W. Buennagel, M. Forster, N. M. Kronenberg, M. Scharber, M. Koppe, M. Morana, C. J. Brabec, K. Meerholz, U. Scherf, Chem. Mater. **20**, 4045 (2008).
[33] L. Liao, L. Dai, A. Smith, M. Durstock, J. Lu, J. Ding, Y. Tao, Macromolecules **40**, 9406 (2007).
[34] C. H. Chen, C. H. Hsieh, M. Dubosc, Y. J. Cheng, C. S. Hsu, Macromolecules **43**, 697 (2010).
[35] J. Ding, N. Song, Z. Li, Chem. Commun. **46**, 8668 (2010).
[36] E. Ahmed, S. Subramaniyan, F. S. Kim, H. Xin, S. A. Jenekhe, Macromolecules **44**, 7207 (2011).
[37] Y. Zhang, J. Y. Zou, C. C. Cheuh, H. L. Yip, A. K. Y. Jen. Macromolecules **45**, 5427 (2012).
[38] Y. J. Cheng, Y. J. Ho, C. H. Chen, W. S. Kao, C. E. Wu, S. L. Hsu, C. S. Hsu. Macromolecules **45**, 2690 (2012).
[39] K. C. Li, J. H. Huang, Y. C. Hsu, P. J. Huang, C. W. Chu, J. T. Lin, K. C. Ho, K. H. Wei, H. C. Lin, Macromolecules **42**, 3681 (2009).
[40] F. Y. Pan, J. G. Yang, H. D. Liang, C. H. Ge, Chin. J. Appl. Chem. **18**, 1000 (2001).
[41] L. T. Pierre, A. N. Boudreault, L. Mario, Chem Mater, **23**, 456 (2011).
[42] G. Lu, H. Usta, C. Risko, L. Wang, A. Facchetti, M. A. Ratner, T. J. Marks, J. Am. Chem. Soc. **130**, 7670 (2008).
[43] R. S. Ashraf, J. Gilot, R. A. J. Janssen, Sol. Energy. Mater. Sol. Cells. **94**, 1759 (2010).
[44] H. P. Shi, L. W. Shi, J. X. Dai, L. Xu, M. H. Wang, X. H. Wu, L. Fang, C. Dong, M. M. F. Choi, Tetrahedron **68**, 9788 (2012).
[45] Z. B. Lim, B. Xue, S. Bomma, H. Li, S. Sun, Y. M. Lam, W. J. Belcher, P. C. Dastoor, A. C. Grimsdale, J Polym Sci Part A: Polym Chem, **49**, 4387 (2011).
[46] X. Guo, H. Xin, F. S. Kim, A. D. T. Liyanage, S. A. Jenekhe, M. D. Watson, Macromolecules, **44**, 269 (2011).
[47] M. C. Scharber, D. Wuhlbacher, M. Koppe, P. Denk, C. Waldauf, A. J. Heeger, C. J. Brabec, Adv. Mater. **18**, 789 (2006).
[48] E. G. Wang, L. T. Hou, Z. Q. Wang, Z. F. Ma, S. Hellström, W. L. Zhuang, F. L. Zhang, O. Inganäs, M. R. Andersson, Macromolecules **44**, 2067 (2011).
[49] Y. F. Li, Y. Cao, J. Gao, D. L. Wang, G. Yu, A. J. Heeger, Synth. Met. **99**, 243 (1999).
[50] J. Pommerehne, H. Vestweber, W. Guss, R. F. Mahrt, H. Bassler, M. Porsch, J. Daub, Adv. Mater. **7**, 551 (1995).
[51] E. J. Zhou, J. Z. Cong, K. Tajima, C. H. Yang, K. Hashimoto, J. Phys. Chem. C, **116**, 2608 (2012).
[52] B. C. Thompson, J. M. J. Frechet, Angew. Chem. Int. Ed. **47**, 58 (2008).

*Corresponding author: qych0422@aliyun.com